

# Influence of modulus, thickness and material type on the mechanical behavior of pavement structures

Hoang Thi Thanh Nhan<sup>1\*</sup>, Nguyen Quang Tuan<sup>1</sup>

<sup>1</sup> University of Transport and Communications

## KEYWORDS

Pavement structure  
Elastic modulus  
Layer thickness  
Tensile strain  
Vertical strain  
Surface deflection

## ABSTRACT

This study investigates the effects of elastic modulus, layer thickness and material type on pavement structures using simulations with the Alizé-LCPC software. Two pavement types were analyzed: (i) flexible and (ii) high-grade pavements. The evaluated indicators include tensile strain at the bottom of the asphalt layer ( $\epsilon_T$ ), vertical strain at the top of the subgrade ( $\epsilon_Z$ ) and surface deflection ( $D_0$ ). The results indicate a nonlinear relationship between asphalt layer thickness and tensile strain, with a “critical thickness zone” where  $\epsilon_T$  reaches its maximum before decreasing as the layer becomes thicker. Asphalt thickness strongly influences all three indicators, while its elastic modulus primarily governs  $\epsilon_T$ . The unbound granular base mainly affects subgrade strain but has limited impact on surface deflection and tensile strain. Pavements with only unbound granular bases show low structural efficiency, whereas high-modulus base layers in high-grade pavements substantially reduce  $\epsilon_T$ ,  $\epsilon_Z$  and  $D_0$ , enhancing overall structural strength and stability.

## 1. Introduction

A pavement structure is a multilayered system designed to distribute stresses and limit deformations under traffic loading. Each layer – including surface and base courses – is specified with particular thicknesses and material properties to ensure sufficient bearing capacity, durability and service life. Among these, the elastic modulus, layer thickness and material type are key parameters controlling the stress–strain response of the pavement structure, thereby affecting the development of common distresses such as fatigue cracking, thermal cracking and rutting.

Fundamental research has highlighted the critical importance of selecting appropriate thicknesses and material properties for each layer. Huang (2004) [1] established the theoretical framework for stress distribution within pavement structures, providing the foundation for subsequent advanced analyses. Building on this work, recent simulation-based studies, including those by Selsal et al. (2022) [2], have examined the effect of surface course thickness on stress and strain distribution, showing that optimizing layer thickness can improve load-bearing capacity and extend pavement service life.

Typical pavement distresses, such as fatigue cracking and rutting, are closely influenced by material type and layer thickness. Suo et al. (2012) [3] demonstrated that incorporating polymers into asphalt concrete enhances fatigue resistance due to improved elastic properties. Additional studies by Sousa et al. (1998) [4], Shafabakhsh et al. (2013) [5], Elshaer and Daniel (2018) [6] and Hadi and Al-Sherrawi (2021) [7] showed that adjusting the thickness and stiffness of base layers can effectively reduce deformations and improve structural stability.

The interplay among material properties, layer thickness and environmental factors (e.g., temperature and moisture) underscores

the need for an optimized design approach to control stresses and deformations throughout the pavement system. Deng et al. (2020) [8] and Khodary et al. (2020) [9] emphasized that a thicker surface layer or one with a higher modulus can substantially reduce deformations under heavy traffic loads. Similarly, Elshaer and Daniel (2018) [6] and Castelló et al. (2020) [10] reported that proper adjustment of layer modulus and thickness can simultaneously enhance load-carrying capacity, minimize surface deflection and mitigate fatigue cracking.

In Vietnam, several studies have investigated the appropriate thickness and modulus values for asphalt concrete and base layers to optimize pavement design and enhance structural performance. Nguyen Tien Sy and Pham Cao Thang (2017) [11] determined asphalt layer thickness based on shear strength, while Pham Viet Hoang and Pham Cao Thang (2016) [12] highlighted the importance of fatigue strength. Pham Huy Khang et al. (2017) [13] used Abaqus software to simulate stress–strain responses in flexible pavement systems, and Le Van Phuc and Hoang Cong Duc (2020) [14] assessed pavement service life under the combined effects of traffic loading and vehicle speed.

Overall, both international and domestic studies underscore that a quantitative analysis of the effects of elastic modulus, layer thickness and material type on pavement mechanical behavior is crucial for identifying an optimal layer configuration that ensures structural efficiency and cost-effectiveness.

## 2. Research methodology

### 2.1. Pavement materials, structures and modeling

This study aimed to evaluate the influence of pavement structural parameters – including material type, layer thickness and elastic modulus – on performance indicators such as surface deflection

\*Corresponding author: ttnhan.hoang@utc.edu.vn

Received 21/10/2025, Revised 07/11/2025, Accepted 10/11/2025

Link DOI: <https://doi.org/10.54772/jomc.v15i02.1157>



and characteristic mechanical strains within the pavement structure. Within the scope of the study, several representative pavement types were selected for analysis. Each structure was modeled as a multilayer system, with the  $i$ -th layer defined by four fundamental parameters: material type ( $M_i$ ), thickness ( $h_i$ ), elastic modulus ( $E_i$ ) and Poisson's ratio ( $\nu_i$ ). When necessary, the material symbol is specified alongside these parameters. The subgrade was represented as a semi-infinite elastic half-space, characterized by two fundamental mechanical parameters: the elastic modulus ( $E_0$ ) and Poisson's ratio ( $\nu_0$ ), as shown in Figure 1.

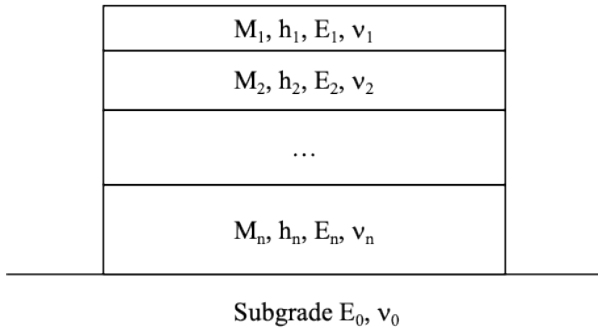


**Figure 1.** Pavement structure model with material layers and mechanical parameters.

The material properties of the pavement layers were selected based on the recommended values provided in contemporary pavement design guidelines, including SETRA-LCPC (France) [15], MEPDG (United States) [16] and Austroads (Australia) [17]. This approach ensures consistency with advanced international design standards, facilitates benchmarking and comparative analysis under Vietnamese conditions.

Numerical simulations were conducted using Alizé-LCPC, a well-established computational tool widely employed for pavement design in France. The applicability of Alizé-LCPC for multilayer pavement analysis has been validated in previous studies, such as Nguyen et al. (2020), which used the software to compute tensile strain in reinforced asphalt pavements [18]. The software enables mechanical analysis of pavement structures based on a multilayer elastic model resting on an elastic half-space, allowing the determination of stresses, strains and deflections at critical locations under standard loading. In this study, all simulations were performed using Alizé R2.3.1. The computational procedure in Alizé comprises two main steps: (i) Definition of material layer parameters, and (ii) Specification of the applied loading conditions.

For all simulations, the applied load corresponded to a standard single-axle load, represented by a uniform contact pressure of 0.6 MPa distributed over a circular area with a diameter of 33 cm. Depending on the material properties of the layers, the interlayer bonding conditions were assumed to be fully bonded, partially bonded or allowing slip.

## 2.2. Problem formulation and objectives

### 2.2.1. Problem 1

Problem 1 was formulated to analyze the structural behavior of a typical flexible pavement commonly used in Vietnam. The modeled pavement structure consists of two asphalt concrete surface layers (denoted as AC1 and AC2) placed over two unbound granular layers (denoted as GNT1 and GNT2), as summarized in Table 1. The computational model was developed to evaluate the influence of design parameters – including the thickness and elastic modulus of the lower surface layer (AC2) and the thickness of the upper granular base layer (GNT1) – on the overall load-bearing performance of the pavement structure.

Within the scope of this study, the variable parameters were defined as follows:

- Thickness of the AC2 layer ( $h_{AC2}$ ): 0, 1, 2, 3, 5, 7, 9 and 11 cm;
- Elastic modulus of the AC2 layer ( $E_{AC2}$ ): 5400, 6000, 7000, 9000, 11000 and 14000 MPa;
- Thickness of the GNT1 layer ( $h_{GNT1}$ ): 0, 8, 15, 24 and 32 cm.

All other material parameters were kept constant according to the values listed in Table 1. A total of 94 computational cases were analyzed, including:

- 40 cases with  $E_{AC2}$  fixed at 5400 MPa, in which the eight thickness values of  $h_{AC2}$  and five thickness values of  $h_{GNT1}$  were varied simultaneously; and
- 54 additional cases considering three  $h_{AC2}$  values (0, 7 and 11 cm) and three  $h_{GNT1}$  values (0, 15 and 32 cm) in combination with six different elastic modulus values of  $E_{AC2}$ .

Three indicators were used to evaluate pavement behavior: (i) Tensile strain at the bottom of the AC layer ( $\epsilon_T$ ); (ii) Vertical strain at the top of the subgrade ( $\epsilon_z$ ); and (iii) Surface deflection ( $D_0$ ).

By simultaneously examining the effects of asphalt layer thickness and modulus together with the granular base thickness, this study explores the interrelationships among these parameters in terms of strain distribution and surface deflection within the pavement structure. The findings provide insights into the balance between enhancing material stiffness (higher modulus) and increasing layer thickness, thereby supporting the development of more rational and performance-based pavement design approaches.

### 2.2.2. Problem 2

Problem 2 extends the analysis to high-grade pavement structures typically used for highways and major urban arterial roads. Unlike Problem 1, in which the pavement included only unbound granular base and subbase layers, this problem investigates the effects of different base types – including bituminous and cement-treated



materials – on the mechanical response and overall load-bearing capacity of the pavement structure.

The modeled pavement structure consists of two fixed surface layers: a porous asphalt concrete layer (denoted BBD<sub>r</sub>) with a thickness of  $h_{\text{BBD}_r} = 4$  cm and an elastic modulus of  $E_{\text{BBD}_r} = 3000$  MPa, and a dense asphalt concrete layer (AC2) with  $h_{\text{AC2}} = 6$  cm and  $E_{\text{AC2}} = 5400$  MPa. These two surface layers were kept constant in all simulation scenarios.

The underlying base and subbase layers (Layers 3 and 4) were varied across different scenarios to represent several typical high-grade pavement configurations, including:

- Typical Vietnamese pavement structure: both the base and subbase layers consist entirely of unbound granular materials.
- Asphalt treated base (ATB) pavement structure: the base layer is replaced with asphalt concrete.
- Semi-rigid pavement structure: the base layer is replaced with cement-stabilized granular material or cement concrete.

- Composite pavement structure: a bituminous base layer and a cement-stabilized granular subbase.

The material symbols and elastic moduli were adopted from the SETRA–LCPC pavement design standards (France) [15] to enable comparison with international design guidelines. For each pavement type, the thicknesses of the base and subbase layers were varied within practical ranges to generate multiple computational scenarios, facilitating the analysis of strain responses and overall structural performance.

The same three indicators as in Problem 1 were used to evaluate the structural response of the pavement system. The objective of this analysis is to examine how these indicators vary with changes in material type and layer thickness in high-grade pavement structures. Poisson's ratio was assumed to be 0.25 for cement concrete and cement-stabilized granular materials, and 0.35 for all other materials.

**Table 1.** Material properties used in Problem 1.

No	Pavement layer	Material type	Symbol	Thickness (h, cm)	Elastic modulus (E, MPa)	Poisson's ratio ( $\nu$ )
1	Surface	Asphalt concrete	AC1	5	5400	0.35
2		Asphalt concrete	AC2	0, 1, 2, 3, 5, 7, 9, 11	5400, 6000, 7000, 9000, 11000, 14000	0.35
3	Base	Unbound granular base	GNT1	0, 8, 15, 24, 32	300	0.35
4	Subbase	Unbound granular subbase	GNT2	30	250	0.35
5	Subgrade			-	50	0.35

**Table 2.** Pavement types and base layer parameters used in Problem 2.

Pavement type	Layer 3 (Base)			Layer 4 (Subbase)		
	Material	Symbol	E (MPa)	Material	Symbol	E (MPa)
Typical Vietnamese	Unbound granular base	GNT1	300	Unbound granular subbase	GNT2	250
Asphalt treated base (ATB)	Asphalt concrete	GB3	9300	Asphalt concrete	GB3	9300
					EME2	14000
		EME2	14000	Unbound granular subbase	GNT2	250
				Asphalt concrete	GB3	9300
Semi-rigid	Cement-stabilized granular	GC3	23000	Unbound granular subbase	GNT2	250
	Cement concrete	BC2	20000			
		BC5	35000			
Composite	Asphalt concrete	GB3	9300	Cement-stabilized granular	GC3	23000

### 3. Results and discussion

#### 3.1. Effects of material and layer thickness on flexible pavement behavior

This section presents and discusses the results of Problem 1, focusing on three parameters: the thickness and elastic modulus of the

lower asphalt concrete layer ( $h_{\text{AC2}}$  and  $E_{\text{AC2}}$ ) and the thickness of the granular base layer ( $h_{\text{GNT1}}$ ). The combined effects of these parameters on the main mechanical response indicators are analyzed below.

##### 3.1.1. Effect of asphalt concrete layer thickness



The results indicate that the thickness of the lower asphalt concrete layer ( $h_{AC2}$ ) significantly affects the mechanical responses of the flexible pavement structure, including the tensile strain at the bottom of the asphalt layer ( $\epsilon_T$ ), the vertical strain at the top of the subgrade ( $\epsilon_Z$ ) and the surface deflection ( $D_0$ ).

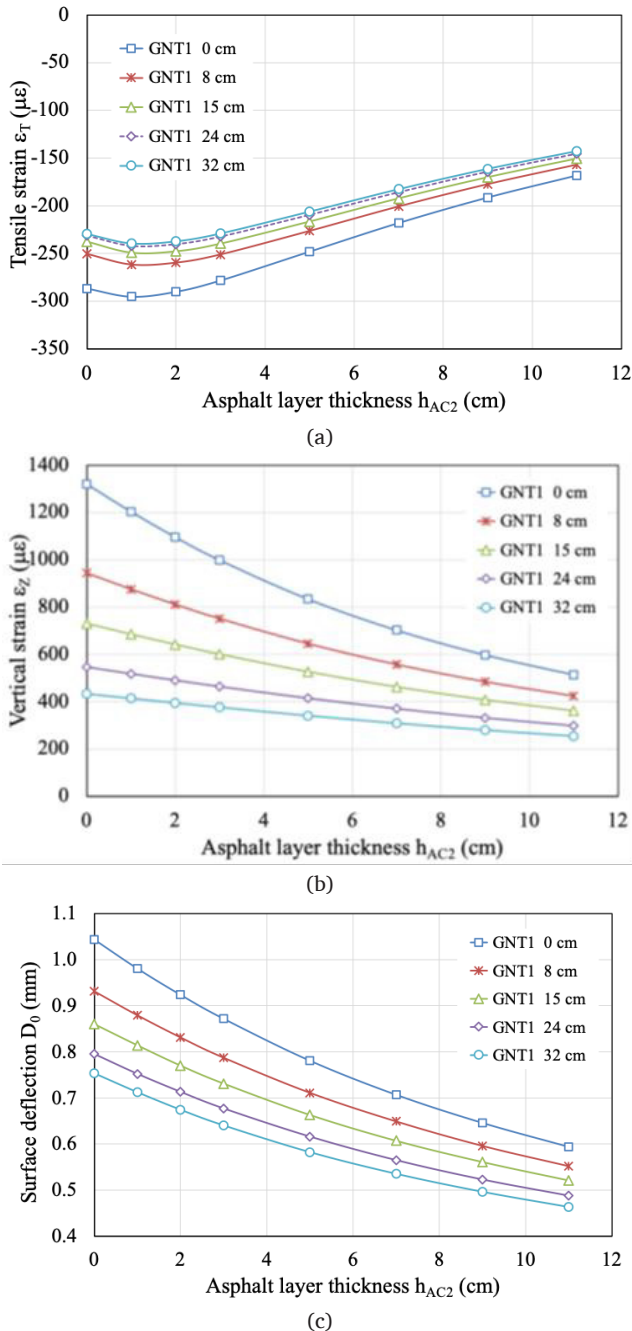


**Figure 2.** Effect of the asphalt concrete layer thickness ( $h_{AC2}$ ) on (a) tensile strain  $\epsilon_T$ , (b) vertical strain  $\epsilon_Z$ , and (c) surface deflection  $D_0$ , for  $E_{AC2} = 5400$  MPa, with varying thicknesses of the granular base layer ( $h_{GNT1}$ ).

For a constant elastic modulus ( $E_{AC2}$ ), increasing the thickness  $h_{AC2}$  results in a nonlinear variation of the tensile strain ( $\epsilon_T$ ) (Figure 2a). At the initial stage, as  $h_{AC2}$  increases from 0 to approximately 1 cm,  $\epsilon_T$  slightly rises and reaches its peak at around  $h_{AC2} \approx 1$  cm (corresponding to a total asphalt thickness of about 6 cm). This range may be considered a critical thickness zone, where a modest increase in asphalt thickness causes a temporary rise in tensile stress before the overall decreasing trend begins. Beyond this threshold,  $\epsilon_T$  decreases steadily with further increases in asphalt thickness. When  $h_{AC2} \geq 3$  cm, the reduction becomes nearly linear, averaging approximately 6–7 % per additional centimeter of asphalt layer thickness. In the most unfavorable configuration ( $h_{GNT1} = 0$  cm),  $\epsilon_T$  decreases by approximately 43 %, while in the pavement with the thickest base layer ( $h_{GNT1} = 32$  cm), the reduction remains around 40 %.

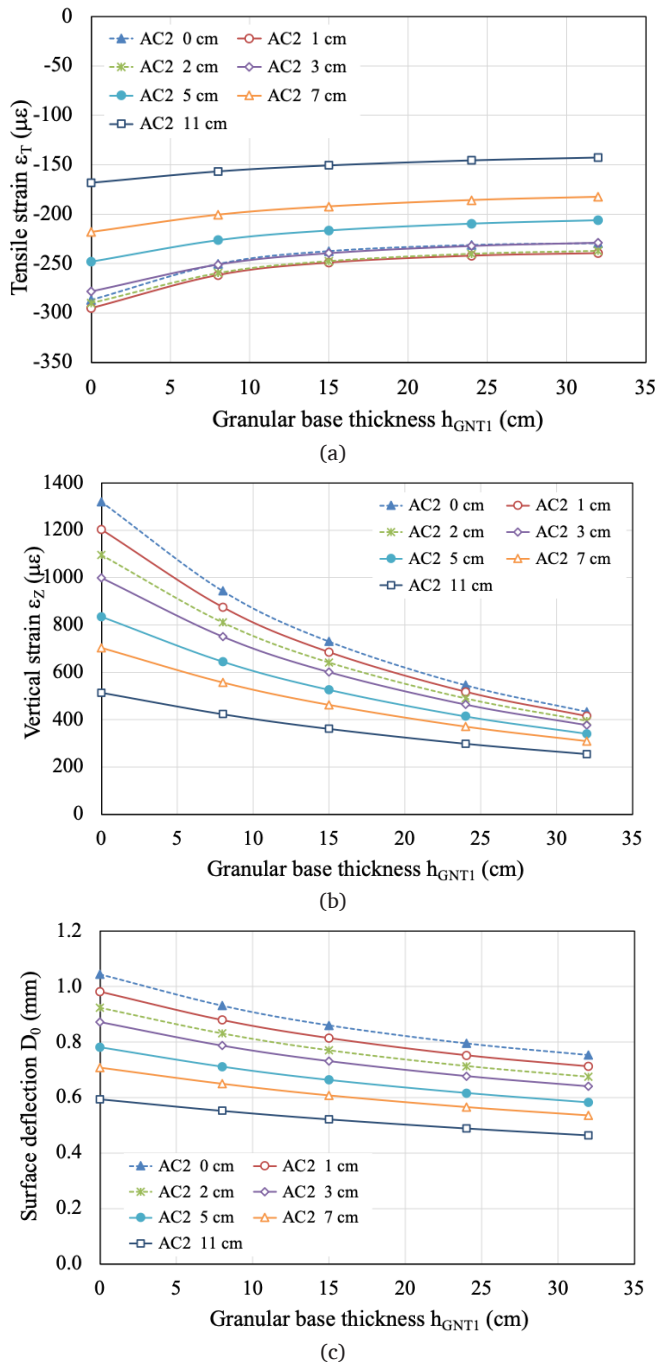
Similarly, the vertical strain at the top of the subgrade ( $\epsilon_Z$ ) decreases significantly – and more sensitively than  $\epsilon_T$  – as the asphalt layer thickness  $h_{AC2}$  increases (Figure 2b). In the absence of a granular base layer ( $h_{GNT1} = 0$ ),  $\epsilon_Z$  decreases by approximately 61 % when  $h_{AC2}$  increases from 0 to 11 cm. The corresponding reductions are about 55 %, 50 % and 41 % for  $h_{GNT1}$  values of 8, 15 and 32 cm, respectively. These results indicate that even with a thicker granular base, the strain-reducing effect of the asphalt layers remains substantial, though its magnitude gradually diminishes. Overall,  $\epsilon_Z$  exhibits an almost linear decrease for  $h_{AC2} \geq 3$  cm, with an average reduction rate of about 6–8 % per additional centimeter of asphalt layer thickness.

Figure 2c shows that the surface deflection ( $D_0$ ) decreases consistently with increasing  $h_{AC2}$ . This downward trend remains stable across all configurations and becomes nearly linear for  $h_{AC2} \geq 3$  cm. For the pavement without a granular base layer ( $h_{GNT1} = 0$  cm),  $D_0$  decreases by approximately 43 % as  $h_{AC2}$  increases from 0 to 11 cm. In pavements with granular base layers,  $D_0$  decreases slightly less – by about 41 %, 39 % and 38 % for  $h_{GNT1}$  values of 8, 15 and 32 cm, respectively.

### 3.1.2. Effect of granular base layer thickness

The results indicate that as the thickness of the unbound granular base layer ( $h_{GNT1}$ ) increases from 0 to 32 cm, the tensile strain at the bottom of the asphalt layer ( $\epsilon_T$ ) slightly decreases (Figure 3a). This behavior is mechanically reasonable because the granular base layer distributes the applied load, thereby reducing the concentration of tensile stress at the bottom of the asphalt layer. The tensile strain  $\epsilon_T$  decreases by approximately 14–20 %, depending on the thickness of the lower asphalt layer ( $h_{AC2}$ ). Specifically, when  $h_{AC2} = 0$ –3 cm, increasing  $h_{GNT1}$  produces the greatest reduction in  $\epsilon_T$  (about 18–20 %); when  $h_{AC2} = 5$ –7 cm, the reduction remains noticeable but slightly smaller (around 16–17 %); and when  $h_{AC2} = 9$ –11 cm, the reduction drops to about 14–15 %, as the asphalt layers are already stiff enough to carry most of the applied load.





**Figure 3.** Effect of granular base layer thickness ( $h_{GNT1}$ ) on (a) tensile strain  $\epsilon_T$ , (b) vertical strain  $\epsilon_z$ , and (c) surface deflection  $D_0$ , for  $E_{AC2} = 5400$  MPa, with varying thicknesses of lower asphalt layer thicknesses ( $h_{AC2}$ ).

These results confirm that both the asphalt concrete thickness ( $h_{AC2}$ ) and the granular base thickness ( $h_{GNT1}$ ) have a significant influence on the tensile strain at the bottom of the asphalt layer. Notably, a clear correlation between these two parameters is observed across different pavement configurations. The tensile strain  $\epsilon_T$  remains nearly constant when an increase of 1 cm in asphalt concrete

corresponds to an 8–9 cm increase in the granular base. For instance, pavement structures with combined thicknesses of  $h_{AC2} + h_{GNT1} = 1 + 32$  cm,  $2 + 24$  cm, and  $3 + 15$  cm yield nearly identical  $\epsilon_T$  values (approximately 239–240  $\mu\epsilon$ ). This finding demonstrates that the strain-reduction efficiency of asphalt concrete is considerably higher than that of the granular base, with an equivalent effectiveness ratio of about 1:8.

As shown in Figure 3b, the vertical strain at the top of the subgrade ( $\epsilon_z$ ) decreases significantly as the granular base thickness ( $h_{GNT1}$ ) increases. This trend is consistent across all asphalt layer thicknesses ( $h_{AC2}$ ). When  $h_{GNT1}$  increases from 0 to 32 cm,  $\epsilon_z$  decreases on average by about 55–65 %, depending on  $h_{AC2}$ . The largest reductions occur in pavements with thinner asphalt layers, where  $\epsilon_z$  drops by more than 60 %, highlighting the granular base's key role in distributing vertical stresses and limiting load transfer to the subgrade. Conversely, as the asphalt layer becomes thicker, the reduction in  $\epsilon_z$  due to an increased granular base thickness becomes smaller, as a portion of the load is already carried by the asphalt layers.

The surface deflection ( $D_0$ ) follows a similar trend: it decreases by approximately 22–28 % as  $h_{GNT1}$  increases from 0 to 32 cm, with the greatest reductions observed in pavements with thinner asphalt layers (Figure 3c). These results demonstrate that increasing the granular base thickness substantially enhances the overall stiffness of the pavement structure, thereby reducing both subgrade deformation and surface deflection.

### 3.1.3. Effect of elastic modulus

The results show that increasing the elastic modulus of the asphalt concrete layer ( $E_{AC2}$ ) significantly reduces the tensile strain at the bottom of the asphalt layer ( $\epsilon_T$ ), with an average decrease of about 30–40 % (Figure 4a). This trend is consistent across all structural configurations and is relatively insensitive to variations in asphalt thickness ( $h_{AC2}$ ) or granular base thickness ( $h_{GNT1}$ ), indicating that the effect of  $E_{AC2}$  is dominant and largely independent of geometric factors.

When comparing the effects of increasing the asphalt modulus versus increasing the granular base thickness, increasing the asphalt modulus produces a more pronounced reduction in tensile strain within the studied range. For example, with an asphalt thickness of 7 cm, raising  $E_{AC2}$  from 5400 to 14000 MPa reduces  $\epsilon_T$  by about 35%, whereas increasing  $h_{GNT1}$  from 0 to 32 cm yields only a 16 % reduction. A similar trend is observed for an 11 cm asphalt layer, where  $\epsilon_T$  decreases by roughly 40% due to the higher modulus, compared to about 15 % from a thicker granular base. For a moderate modulus increase – from 9000 to 11000 MPa ( $\approx 20$  %) – the resulting reduction in  $\epsilon_T$  is approximately equivalent to adding 15 cm of granular base. This relationship holds for both  $h_{AC2} = 7$  cm and  $h_{AC2} = 11$  cm, indicating that, within the examined material and thickness range, a 20 % increase in asphalt modulus achieves a tensile strain reduction comparable to that of adding 15 cm of granular base.



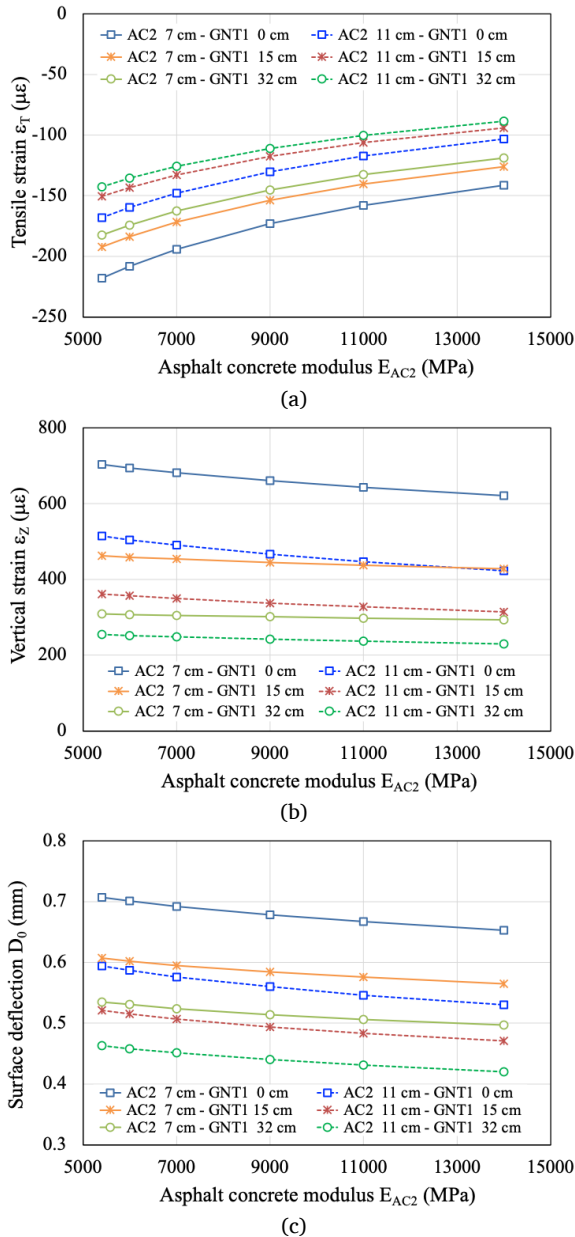


**Figure 4.** Effect of asphalt concrete modulus ( $E_{AC2}$ ) on (a) tensile strain  $\epsilon_T$ , (b) vertical strain  $\epsilon_Z$ , and (c) surface deflection  $D_0$ , for various thicknesses of the lower asphalt layer and granular base layer.

Comparing the effects of increasing modulus versus increasing asphalt thickness highlights a trade-off between stiffness and layer thickness in controlling tensile strain. With a granular base thickness

of 32 cm, a pavement with  $h_{AC2} = 7$  cm and  $E_{AC2} = 11000$  MPa exhibits nearly the same  $\epsilon_T$  as a pavement with  $h_{AC2} = 11$  cm and  $E_{AC2} = 6000$  MPa. This indicates that, within the studied range, an approximately 80 % increase in modulus can achieve a tensile strain reduction comparable to increasing the asphalt layer thickness by about 4 cm.

The vertical strain at the top of the subgrade ( $\epsilon_Z$ ) also decreases as  $E_{AC2}$  increases, though the reduction is much smaller than that observed for  $\epsilon_T$ . In the same range, increasing  $E_{AC2}$  from 5400 to 14000 MPa reduces  $\epsilon_Z$  by only 12–13 % (Figure 4b). This suggests that the asphalt modulus affects subgrade deformation primarily in an indirect manner, as most of the vertical load is transmitted and distributed through the base layers. The influence of  $E_{AC2}$  on  $\epsilon_Z$  becomes noticeable only when the granular base is relatively thin; conversely, with a granular base thickness of around 32 cm,  $\epsilon_Z$  remains nearly constant despite changes in  $E_{AC2}$ .

Surface deflection ( $D_0$ ) shows a modest decrease with increasing asphalt modulus, averaging about 8–9 % (Figure 4c). This behavior reflects the composite nature of  $D_0$ , which represents the overall elastic response of the pavement structure and is influenced by the stiffness and thickness of all layers. Consequently, while increasing  $E_{AC2}$  improves surface stiffness, its impact on  $D_0$  is limited, as the overall deflection is primarily controlled by the mechanical properties of the base layers and subgrade.

### 3.2. Mechanical behavior of high-grade pavement structures

This section examines a series of high-grade pavement structures, including configurations with unbound granular bases, bituminous bases and cement-stabilized or cement concrete base, as presented in Table 2. A reference structure was selected, featuring an upper bituminous base layer (GB3) and a lower unbound granular subbase layer (GNT2), with its configuration and mechanical properties summarized in Table 3. This high-grade pavement structure is currently applied in several expressway projects in Vietnam (e.g., the Hanoi–Hai Phong Expressway), with a total asphalt thickness of approximately 25 cm.

The reference values for the selected pavement structure, calculated under the standard axle load described earlier, are summarized in Table 4. They provide a baseline for comparison and show how  $\epsilon_T$ ,  $\epsilon_Z$  and  $D_0$  change with variations in the material or thickness of the base layers in high-grade pavements.

**Table 3.** Reference pavement structure.

Layer	Material	Thickness, h (cm)	Elastic modulus, E (MPa)
Base (Layer 3)	Bituminous concrete (GB3)	15	9300
Subbase (Layer 4)	Unbound granular subbase (GNT2)	17	250



**Table 4.** Mechanical properties of the reference pavement under standard axle load.

Indicators	Symbol	Reference value
Tensile strain at the bottom of the asphalt layer	$\varepsilon_T$	-83.3 me
Vertical strain at the top of the subgrade	$\varepsilon_z$	332.2 me
Surface deflection	$D_0$	0.456 mm

### 3.2.1. Tensile strain at the bottom of the asphalt layer ( $\varepsilon_T$ )

Figure 5a summarizes the calculated tensile strain at the bottom of the asphalt layer ( $\varepsilon_T$ ) for different combinations of base materials (denoted as Base-Subbase) and layer thicknesses. The results indicate that  $\varepsilon_T$  is strongly affected by both the elastic modulus and thickness of the base layers, with the upper base layer exerting the dominant influence.

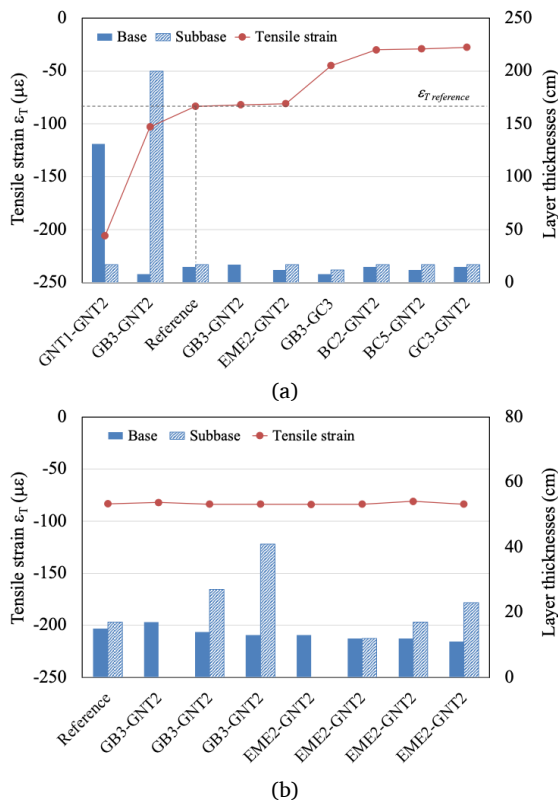


**Figure 5.** Effect of base material and thickness on tensile strain at the bottom of the asphalt layer ( $\varepsilon_T$ ): (a) Relationship between  $\varepsilon_T$  and base thickness; (b) Pavement structures with equivalent  $\varepsilon_T$  values.

When the upper base layer in the reference structure is replaced with an unbound granular base ( $E = 300$  MPa), which has a much lower modulus than the asphalt-treated base GB3 ( $E = 9300$  MPa),  $\varepsilon_T$  increases substantially. Even when the thickness of the unbound granular base exceeds 1.3 m,  $\varepsilon_T$  remains more than 2.4 times greater than that of the reference pavement with a GB3 base. In cases where an 8 cm GB3 layer is retained – similar to thin asphalt-treated base

systems used in expressways – and the underlying unbound granular subbase is thickened from 45 to 200 cm,  $\varepsilon_T$  still shows minimal improvement. These results indicate that increasing the thickness of unbound granular layers, even to the meter scale, offers only limited effectiveness in reducing tensile strain  $\varepsilon_T$ .

In contrast, increasing the thickness of the asphalt-treated base (GB3) results in a clear improvement. When its thickness increases from 15 cm to 17 cm, the structure can completely eliminate the unbound granular subbase while maintaining  $\varepsilon_T$ ,  $\varepsilon_z$  and  $D_0$  values nearly identical to those of the reference pavement with a 17 cm granular subbase. Based on these findings, an empirical relationship can be established: 1 cm of GB3 asphalt-treated base is approximately equivalent to 8–9 cm of unbound granular subbase in controlling strain and deflection. When a stiffer asphalt-treated base (EME2,  $E = 14000$  MPa) is used instead of GB3,  $\varepsilon_T$  decreases slightly, allowing a 2–3 cm reduction in total asphalt thickness while maintaining comparable  $\varepsilon_T$  values.

The reduction in  $\varepsilon_T$  becomes particularly pronounced when the base layer is replaced with higher-modulus materials such as cement-stabilized granular (GC3,  $E = 23000$  MPa) or cement concrete (BC2,  $E = 20000$  MPa; BC5,  $E = 35000$  MPa). In these cases,  $\varepsilon_T$  decreases markedly compared with pavements using GB3 or unbound granular bases. Notably, when BC5 is used as the upper base,  $\varepsilon_T$  is reduced by more than 60% relative to the reference pavement with GB3 (with identical subbase conditions), underscoring the dominant influence of base stiffness on tensile-strain performance.

Figure 5b illustrates structural configurations that exhibit  $\varepsilon_T$  values equivalent to the reference structure. The results indicate that several configurations with asphalt-treated bases (GB3 or EME2) can achieve comparable  $\varepsilon_T$  levels by adjusting the thickness of the unbound granular subbase. For instance, when a high-modulus asphalt-treated base EME2 ( $E = 14000$  MPa) is used, the asphalt layer thickness can be reduced to about 11 cm, while increasing the granular subbase layer to around 20 cm maintains  $\varepsilon_T$  comparable to the reference structure with GB3. For pavements incorporating a cement-stabilized granular base (GC3) or cement concrete bases (BC2, BC5),  $\varepsilon_T$  values are so low that no equivalent combinations appear in the comparison.

### 3.2.2. Vertical strain at the top of the subgrade ( $\varepsilon_z$ )

The analysis results indicate that the vertical strain at the top of the subgrade ( $\varepsilon_z$ ) decreases as the total thickness of the base layers



increases. For pavement structures where both the upper and lower base layers consist of unbound granular materials ( $E = 300$  and  $250$  MPa, respectively),  $\varepsilon_z$  decreases rapidly when the total base thickness is less than about  $1.0$  m. However, once the thickness reaches approximately  $1.5$  m, the rate of decrease becomes minimal, suggesting that additional thickness provides little further benefit (Figure 6a). For pavements with a stiffer upper base layer, such as the asphalt-treated base EME2 ( $E = 14000$  MPa),  $\varepsilon_z$  exhibits a similar decreasing trend as total base thickness increases (Figure 6b). This consistent reduction of  $\varepsilon_z$  aligns with the findings from Problem 1, confirming the stability of vertical load distribution in multilayer pavement systems.

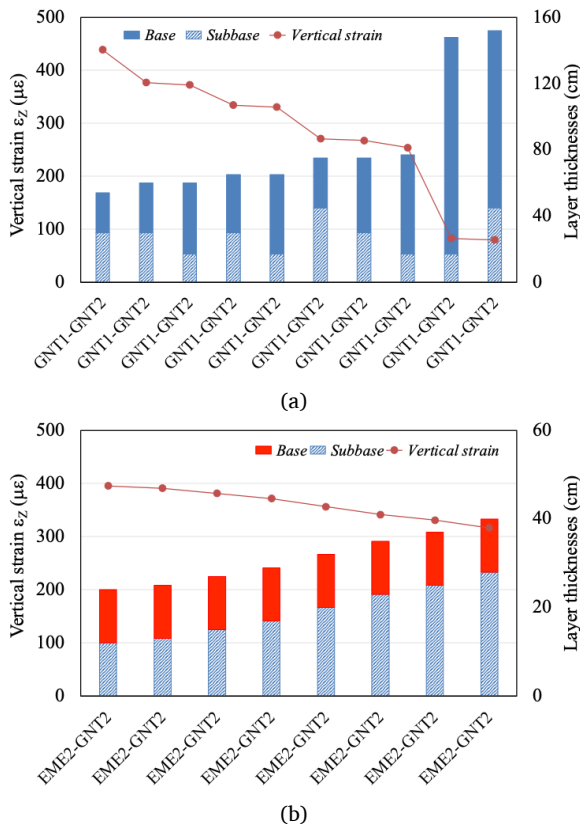


**Figure 6.** Effect of total base thickness on vertical strain at the top of the subgrade ( $\varepsilon_z$ ): (a) Unbound granular base; (b) Asphalt-treated base (EME2).

When analyzing configurations with a fixed unbound granular subbase but varying upper base materials and moduli (Figure 7a), the results indicate that  $\varepsilon_z$  is governed primarily by the total structural thickness rather than by the stiffness of the upper base layer alone. Increasing the modulus of the upper base –from softer materials such as GB3 and EME2 to stiffer ones such as GC3, BC2 or BC5– reduces  $\varepsilon_z$  (Problem 1); however, the reduction becomes significant only when the modulus contrast is substantial or when layer thickness is optimized simultaneously. Conversely, pavement structures

incorporating relatively unbound granular bases can still achieve low  $\varepsilon_z$  values if the overall thickness is sufficiently large. These findings demonstrate that the vertical strain at the top of the subgrade is controlled mainly by the pavement's overall load-distribution capacity rather than by the stiffness of any single layer.

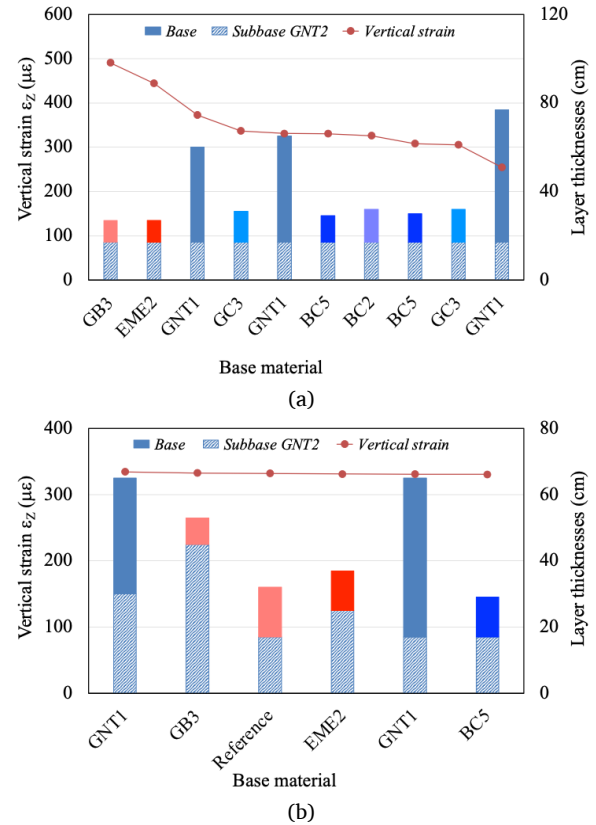


**Figure 7.** Effect of base layers on vertical strain at the top of the subgrade ( $\varepsilon_z$ ): (a) Variation in upper base material; (b) Pavement structures with equivalent  $\varepsilon_z$  values.

Specifically, Figure 7b compares the  $\varepsilon_z$  of the reference structure (GB3 15 cm + GNT2 17 cm) with several alternative configurations. Pavements composed entirely of unbound granular bases (GNT1 and GNT2, with  $E = 300$  and  $250$  MPa, respectively) can achieve comparable  $\varepsilon_z$  values when the total base thickness increases to approximately 65 cm, regardless of how the thickness is distributed between the upper and lower layers. A structure with a thin asphalt-treated base (GB3 8 cm + GNT2 45 cm) also yields similar  $\varepsilon_z$ , indicating that the thickness of a high-stiffness asphalt-treated base (GB3) can be reduced if the granular layer (GNT2) is substantially thickened. Meanwhile, for high-modulus materials such as EME2 or BC5, equivalent  $\varepsilon_z$  values can be achieved even when the total thickness is reduced to about 30–40 cm. Notably, composite structures combining asphalt-treated and cement-stabilized bases produce significantly lower  $\varepsilon_z$  values than the reference structure, demonstrating their superior capacity for vertical load distribution.



Consequently, no composite configuration exhibits  $\varepsilon_z$  values equivalent to that of the reference pavement.

### 3.2.3. Surface deflection ( $D_0$ )

The results show that surface deflection ( $D_0$ ) decreases notably as the thickness or stiffness of the base layers increases, following a trend similar to that of the vertical strain at the top of the subgrade ( $\varepsilon_z$ ). However, since  $D_0$  represents the overall deformation of the entire pavement system – including the surface, base and subgrade layers – its sensitivity is lower than that of  $\varepsilon_z$ .

For pavement structures in which both the base layers consist of unbound granular materials ( $E = 300$  and  $250$  MPa, respectively),  $D_0$  decreases rapidly when the total base thickness is less than about  $1.0$  m. Once the total thickness reaches approximately  $1.5$  m, further increases of a few centimeters provide little additional reduction in deflection, with  $D_0$  values remaining around  $0.45$ – $0.46$  mm (Figure 8a). Pavements with stiffer upper bases – such as asphalt-treated layers (GB3, EME2) or cement-stabilized materials (GC3, BC2, BC5) – exhibit substantially lower  $D_0$  values than those composed entirely of unbound granular layers, reflecting their higher overall stiffness and superior load-distribution capability.

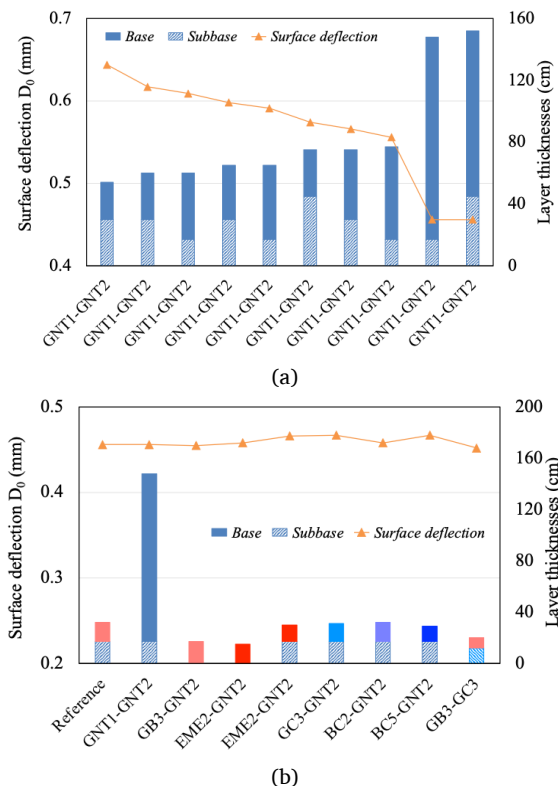


**Figure 8.** Effect of base layers on surface deflection ( $D_0$ ): (a) Relationship between  $D_0$  and total base thickness; (b) Pavement structures with equivalent  $D_0$  values.

Equivalent  $D_0$  values can be achieved through different combinations of materials and layer thicknesses by appropriately balancing stiffness and thickness. Specifically, pavements constructed entirely with unbound granular materials can only reach  $D_0$  values comparable to the reference structure when the total base thickness increases to approximately  $1.5$  m. In contrast, pavements incorporating asphalt-treated, cement-stabilized or composite bases can achieve equivalent  $D_0$  values even with a total thickness of only about  $35$ – $40$  cm (Figure 8b).

## 4. Conclusions

The analyses conducted in this study revealed the relationships among elastic modulus, layer thickness and material type with the mechanical responses of pavement structures, including the tensile strain at the bottom of the asphalt layer ( $\varepsilon_T$ ), the vertical strain at the top of the subgrade ( $\varepsilon_z$ ) and the surface deflection ( $D_0$ ):

- The thickness of the asphalt surface layer ( $h_{AC2}$ ) exhibits a nonlinear influence on  $\varepsilon_T$ . Initially,  $\varepsilon_T$  slightly increases and reaches its maximum at approximately  $h_{AC2} \approx 1$  cm (corresponding to a total asphalt thickness of about  $6$  cm), which can be considered an unfavorable thickness zone. Beyond this point,  $\varepsilon_T$  gradually decreases as the asphalt thickness continues to increase.

- When  $h_{AC2}$  increases from  $0$  to  $11$  cm,  $\varepsilon_T$  decreases by  $40$ – $43$  %,  $\varepsilon_z$  by  $41$ – $61$  %, and  $D_0$  by  $38$ – $43$  %, depending on the thickness of the upper granular base layer ( $h_{GNT1}$  ranging from  $0$  to  $32$  cm).

- Increasing the upper granular base thickness ( $h_{GNT1}$ ) from  $0$  to  $32$  cm further reduces  $\varepsilon_T$  by  $14$ – $20$  %,  $\varepsilon_z$  by  $55$ – $65$  % and  $D_0$  by  $22$ – $28$  %, with more pronounced effects observed in structures with thinner asphalt layers.

- When the elastic modulus of the asphalt layer ( $E_{AC2}$ ) increases from  $5400$  to  $14000$  MPa,  $\varepsilon_T$  decreases on average by  $30$ – $40$  %,  $\varepsilon_z$  by  $12$ – $13$  % and  $D_0$  slightly by  $8$ – $9$  %, reflecting the dominant influence of asphalt stiffness on  $\varepsilon_T$ .

- Comparisons among different base types indicate that pavements with fully unbound granular bases cannot achieve  $\varepsilon_T$  values equivalent to those with asphalt-treated bases, even when the granular base thickness is increased by several meters. Conversely, pavements incorporating asphalt-treated bases can reduce the required base thickness by using asphalt mixtures with higher modulus or by increasing the thickness of the underlying granular base, while maintaining equivalent  $\varepsilon_T$  values. Pavements with cement-stabilized aggregate or cement concrete bases (GC3, BC2, BC5) exhibit substantially lower  $\varepsilon_T$  values; for the BC5 structure in particular,  $\varepsilon_T$  is reduced by more than  $60$  %, indicating that no configuration can match the reference pavement in terms of  $\varepsilon_T$ .

- The vertical strain  $\varepsilon_z$  consistently decreases as the total base thickness increases. Pavements with fully unbound granular bases achieve equivalent  $\varepsilon_z$  values only when the total base thickness reaches approximately  $65$  cm, whereas pavements with stiffer upper



bases (GB3, EME2, GC3, BC2, BC5) can reach equivalent  $\varepsilon_z$  values with total base thicknesses of only 30–40 cm. Composite structures combining asphalt and cement-stabilized base layers produce considerably smaller  $\varepsilon_z$  values; thus, no composite configuration yields  $\varepsilon_z$  equivalent to the reference structure.

- Similarly, the surface deflection  $D_0$  decreases significantly with increasing base thickness. For pavements with fully unbound granular bases, equivalent  $D_0$  values are obtained only when the total base thickness approaches 1.5 m. In contrast, pavements with stiffer upper bases (GB3, EME2, GC3, BC2, BC5) achieve equivalent  $D_0$  values with total base thicknesses of merely 15–30 cm, depending on the material type.

These findings provide practical insights into optimizing pavement layer composition and thickness to balance structural performance and cost efficiency. The simulation-based approach can also be applied to various pavement types and materials to support more reliable performance-based designs. However, as the analysis assumes linear-elastic conditions, future studies should include field validation and viscoelastic or fatigue modeling to better reflect real pavement behavior.

## Acknowledgment

This research is funded by University of Transport and Communications (UTC) under grant number T2025-CT-003.

## References

- [1]. Y. H. Huang, *Pavement Analysis and Design*, 2nd ed. Upper Saddle River, NJ, USA: Pearson Prentice Hall, 2004.
- [2]. Z. Selsal, A. Karakas, and B. Sayin, "Effect of pavement thickness on stress distribution in asphalt pavements under traffic loads," *Case Studies in Construction Materials*, vol. 16, p. e01107, 2022. doi: 10.1016/j.cscm.2022.e01107.
- [3]. Z. Suo, W. G. Wong, X. H. Luo, and B. Tian, "Evaluation of fatigue crack behavior in asphalt concrete pavements with different polymer modifiers," *Construction and Building Materials*, vol. 27, no. 1, pp. 117–125, 2012. doi: 10.1016/j.conbuildmat.2011.08.017.
- [4]. J. B. Sousa, J. C. Pais, M. Prates, R. Barros, P. Langlois, and A.-M. Leclerc, "Effect of aggregate gradation on fatigue life of asphalt concrete mixes," *Transportation Research Record: Journal of the Transportation Research Board*, vol. 1630, no. 1, pp. 62–68, 1998. doi: 10.3141/1630-08.
- [5]. G. A. Shafabakhsh, M. Motamedi, and A. Famili, "Influence of asphalt concrete thickness on settlement of flexible pavements," *Electronic Journal of Geotechnical Engineering*, vol. 18, pp. 473–483, 2013.
- [6]. M. Elshaer and J. S. Daniel, "Impact of pavement layer properties on the structural performance of inundated flexible pavements," *Transportation Geotechnics*, vol. 16, pp. 11–20, 2018. doi: 10.1016/j.trgeo.2018.06.002.
- [7]. M. A. S. Hadi and M. H. Al-Sherrawi, "The influence of base layer thickness in flexible pavements," *Engineering, Technology & Applied Science Research*, vol. 11, no. 6, pp. 7904–7909, 2021. doi: 10.48084/etasr.4573.
- [8]. C. Deng, Y. Jiang, Z. Han, H. Lin, and J. Fan, "Effects of paving technology, pavement materials, and structures on the fatigue property of double-layer pavements," *Advances in Materials Science and Engineering*, Article ID 5038370, 2020. doi: 10.1155/2020/5038370.
- [9]. F. Khodary, H. Akram, and N. Mashaan, "Behaviour of different pavement types under traffic loads using finite element modelling," *International Journal of Civil Engineering and Technology*, vol. 11, no. 11, pp. 40–48, 2020.
- [10]. D. L. Castelló, T. G. Segura, L. M. Domingo, A. S. Benlloch, and E. Pellicer, "Influence of pavement structure, traffic, and weather on urban flexible pavement deterioration," *Sustainability*, vol. 12, no. 22, p. 9717, 2020. doi: 10.3390/su12229717.
- [11]. T. S. Nguyễn and P. C. Thăng, "Tính toán lựa chọn chiều dày hợp lý lớp bê tông nhựa theo chỉ tiêu độ bền cắt trượt trong kết cấu áo đường mềm đường ô tô," *Tạp chí Giao thông Vận tải*, 2017.
- [12]. P. V. Hoàng and P. C. Thăng, "Tính toán lựa chọn chiều dày hợp lý lớp bê tông nhựa theo chỉ tiêu độ bền mỏi trong kết cấu áo đường mềm đường ô tô," *Tạp chí Giao thông Vận tải*, 2016.
- [13]. P. H. Khang, N. B. Tùng, and N. Đ. Chung, "Ứng dụng phần mềm Abaqus tính ứng suất, biến dạng kết cấu mặt đường mềm sân bay," *Tạp chí Giao thông Vận tải*, 2017.
- [14]. L. V. Phúc and H. C. Đức, "Đánh giá tuổi thọ kết cấu áo đường mềm chịu ảnh hưởng của tải trọng và vận tốc bằng phương pháp cơ học thực nghiệm," *Tạp chí Giao thông Vận tải*, 2020.
- [15]. SETRA–LCPC, *Guide technique: Conception et dimensionnement des structures de chaussées*. Paris, France: Laboratoire Central des Ponts et Chaussées, 1994.
- [16]. AASHTO, *Mechanistic-Empirical Pavement Design Guide (MEPDG)*. Washington, DC, USA: American Association of State Highway and Transportation Officials, 2008.
- [17]. Austroads, *Guide to Pavement Technology – Part 2: Pavement Structural Design (AGPT02-17)*. Sydney, Australia: Austroads Ltd., Dec. 2017.
- [18]. M. L. Nguyen, C. Chazallon, M. Sahli, G. Koval, and P. Hornych, "Design of reinforced pavements with glass fiber grids: from laboratory evaluation of the fatigue life to accelerated full-scale test," in *Accelerated Pavement Testing to Transport Infrastructure Innovation*, A. Chabot, P. Hornych, J. T. Harvey, and L. G. Loria-Salazar, Eds., Lecture Notes in Civil Engineering, vol. 96. Cham, Switzerland: Springer, 2020, pp. 329–338. doi: 10.1007/978-3-030-55236-7\_34.